



The synthesis and NLO properties of 1,8-naphthalimide derivatives for both femtosecond and nanosecond laser pulses

Gao-Jie Ye^a, Ting-Ting Zhao^b, Zheng-Neng Jin^a, Pei-Yang Gu^a, Jia-Yuan Mao^a, Qing-Hua Xu^b,
Qing-Feng Xu^{a,*}, Jian-Mei Lu^{a,*}, Na-Jun Li^a, Yin-Ling Song^c

^a Key Laboratory of Organic Synthesis of Jiangsu Province, College of Chemistry, Chemical Engineering and Materials Science, Soochow University(Dushuhu Campus), Suzhou, Jiangsu 215123, PR China

^b Department of Chemistry, National University of Singapore, 3 Science Drive 3, Singapore 117543, Singapore

^c Key Laboratory of Optics of Jiangsu Province, College of Physics and Technology, Soochow University(Central Campus), Suzhou, Jiangsu 215006, PR China

ARTICLE INFO

Article history:

Received 11 October 2011

Received in revised form

30 December 2011

Accepted 3 January 2012

Available online 30 January 2012

Keywords:

1,8-Naphthalimide

Hydrazone group

Optical limiting

Excited-state absorption (ESA)

Two-photon absorption (TPA)

Pump probe

ABSTRACT

Four 1,8-naphthalimide derivatives were synthesized for new nonlinear optical(NLO) materials. Hydrazone group as a p- π structure was introduced into the molecule to extend conjugation and produce NLO properties. Their linear and nonlinear optical (NLO) properties were studied in details. The results show that these compounds possess strong excited-state absorption (ESA) properties and optical limiting with nanosecond laser pulses at 532 nm. Moreover, they also preserve the luminescence originated from naphthalimide and two-photon absorption (TPA) behaviour which can be observed under femtosecond laser pulses ranged from 750 to 870 nm. The broad-band optical limiting properties of these compounds indicate that they can be potentially applied in optical limiting materials.

© 2012 Elsevier Ltd. All rights reserved.

1. Introduction

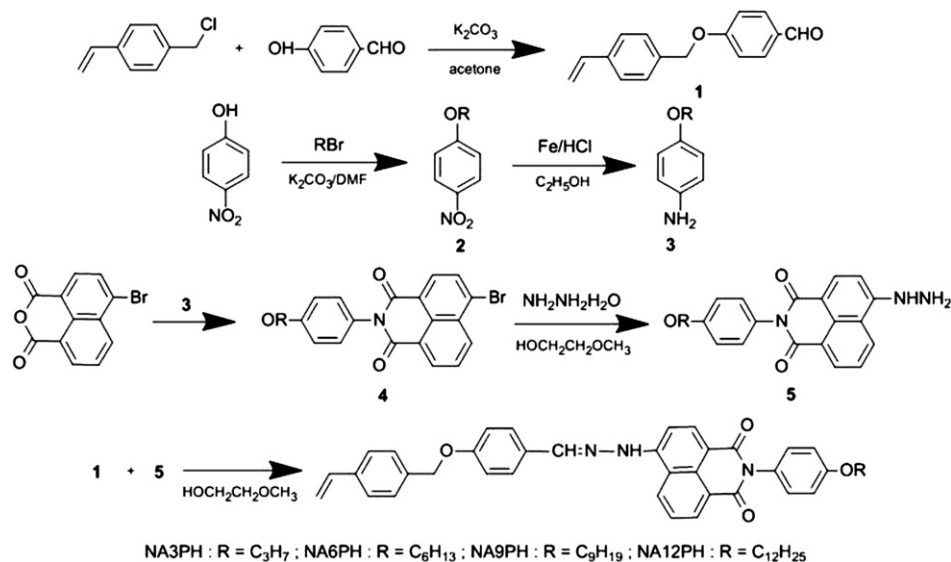
The synthesis of new nonlinear optical (NLO) materials is fundamental in the development of optoelectronic technologies. Due to the low cost, easy fabrication and large NLO susceptibility, organic materials with NLO properties are candidates for potential applications in optical switching, computing, bistable elements, optical limiting (OL) and logic devices [1–7]. Among these applications, optical limiting is one crucial important in the protection of optical sensors or human eyes from laser beams. Optical limiter requires that transmission of the substance is high at low-intensity light but low instantly when exposed to intense laser radiation. Optical limiting of organic materials mainly originates from nonlinear absorption under laser irradiation, whose mechanism includes excited-state absorption (ESA) [8–10] and two-photon absorption (TPA), etc. [11–13]. Fullerenes (C₆₀) and phthalocyanine complexes are commonly considered as classical excited-state

absorption (ESA) materials at high energy end of the visible (400–600 nm). Recently, optical limiting of fluorescent conjugated molecules caused by two-photon absorption (TPA) at the low energy end of the visible (600–800 nm) have attracted much attention. For example, Tavarekere and coworkers [8] found that core-modified expanded porphyrins with large third-order nonlinear optical response at low energy area; Xu et al. [10] investigated the optical limiting property of a new fluorenyl-based chromophore, whose mechanism is attributed to TPA. However, most of the studies are focused on the OL properties at a certain band of laser, the broad-band OL of organic materials properties are studied relatively few. It's probably due to the lack of suitable NLO materials. To obtain a broad-band optical limiter covering the whole visible region, Spangler [14] first suggested to design OL chromophores in a bimechanistic fashion: (1) ESA behaviour at high energy of the visible (400–600 nm) and (2) TPA behaviour at the low energy of the visible (600–800 nm) [15,16]. Till now, few pure organic dyes with such properties have been reported.

Inspired by this idea, we select some usual fluorescent dyes as original chromophores. As a result, the 1,8-naphthalimide derivatives have been extensively used in the dye industry as strongly

* Corresponding authors. Tel.: +86 512 65880367; fax: +86 512 65882875.

E-mail addresses: xuqingfeng@suda.edu.cn (Q.-F. Xu), lujm@suda.edu.cn, jianmeilu_group@hotmail.com (J.-M. Lu).



Scheme 1. Preparation of NAxPHs.

absorbing dyes [17,18], novel therapeutics [19,20], as well as the backbone of chemical probes [21,22]. Meanwhile hydrazone group of the $-\text{CH}=\text{N}-\text{NH}-$ functionality own good hole transport property for technical applications in organic semiconductor designing [23,24]. Its simple synthesis and low cost are the advantages against other classes of charge transport materials.

In this paper, Four 1,8-naphthalimide derivatives containing hydrazone group with different alky chains have been synthesized. The new derivatives based on hydrazone group with a $p-\pi$ structure exhibit good NLO absorption and optical limiting properties. However, the unmodified 1,8-naphthalimide molecule has no NLO absorption effect using nanosecond laser pulses at 532 nm. Furthermore, due to the fluorescence of these compounds preserved at about 550 nm, their TPA properties were also observed by using femtosecond laser pulses ranged from 750 to 870 nm.

2. Sample preparation and experiments

2.1. Materials

4-Vinyl benzyl chloride (90%), P-hydroxybenzaldehyde (99.9%), P-nitrophenol (99.5%), Brominated alkanes (99%), iron powder

reduced (98%), 4-bromo-1,8-naphthalene anhydride (90%), Hydrazine hydrate (85%), Potassium carbonate (99%), Sodium hydroxide (96%), anhydrous magnesium sulphate (98%) were purchased from Shanghai Sinopharm. All reagents used as received without further purification.

2.2. Instruments

^1H NMR spectra were collected on an INVOA 400 Hz NMR spectrometer. Tetramethylsilane was used as the internal reference for the NMR analyses and CDCl_3 as solvent. Elementary analyses were conducted on a Carlo Erba-MOD1106 elementary analysis apparatus. UV–vis spectra were recorded on a Perkin–Elmer λ -17 spectrometer using a 1 cm square quartz cell. The fluorescence spectra were measured on Edinburgh-920 fluorescence spectra photometer (Edinburgh Co. UK) with a slit of 1 nm.

2.3. Preparation of NAxPHs

The intermediate products were synthesized according to the literature methods [25–27] as shown in Scheme 1. 10 mmol of

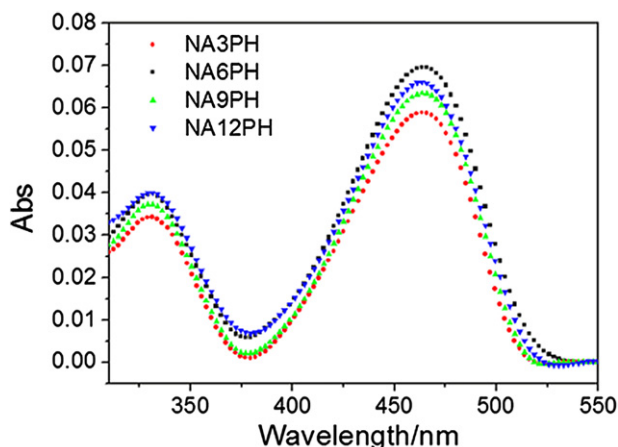


Fig. 1. UV–vis spectra of NAxPHs in DMF.

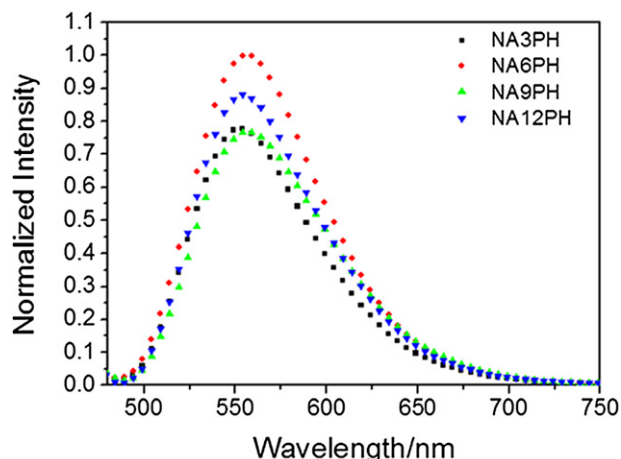


Fig. 2. Fluorescent spectra of NAxPHs in DMF.

Table 1
Photophysical properties of **NA3PH**, **NA6PH**, **NA9PH** and **NA12PH**.

Compounds	$\lambda_{\max}^a/\text{nm}$	$\lambda_{\max}^b/\text{nm}$	$\epsilon^c/\text{mol}^{-1}\text{L}^{-1}\text{cm}^{-1}$	ϕ^d	$\delta_{\max}^e/\text{GM}$	τ^f/ns
NA3PH	464	554	2.20×10^4	0.16	90	1.68
NA6PH	464	554	2.41×10^4	0.19	65	1.69
NA9PH	464	554	2.24×10^4	0.17	77	1.66
NA12PH	464	554	2.28×10^4	0.19	64	1.71

a, b: liner absorption and one-photon fluorescence maxima peak, respectively. c: molar absorption coefficient. d: fluorescence quantum yield. e: the maximum two-photon cross section. f: fluorescence lifetime.

4-hydrazino-N-(4-alkoxy)-phenyl-1,8-naphthalimide and 12 mmol of 4-(4-benzyloxy-vinyl) benzaldehyde were refluxed for 4 h and then cooled to room temperature. The product was obtained by column chromatography with chloroform and ethylacetate.

NA3PH: yield: 46%. $^1\text{H NMR}$ (CDCl_3 , 400 MHz) δ (ppm): 8.86 (s, 1H), 8.63 (m, 2H), 8.27 (s, 1H), 8.01 (s, 1H), 7.85 (d, 1H), 7.70 (t, 3H), 7.46 (m, 4H), 7.21 (d, 2H), 7.01 (m, 4H), 6.76 (m, 1H), 5.81 (d, 1H), 5.31 (d, 1H), 5.14 (s, 1H), 3.92 (t, 2H), 1.83 (m, 2H), 1.06 (t, 3H). Elem. Anal. Calcd. for $\text{C}_{37}\text{H}_{31}\text{N}_3\text{O}_4$: C, 76.40; H, 5.37; N, 7.22; Found: C, 76.43; H, 5.41; N, 7.26. Mp: 265–267 °C.

NA6PH: yield: 51%. $^1\text{H NMR}$ (CDCl_3 , 400 MHz) δ (ppm): 8.83 (s, 1H), 8.63 (m, 2H), 8.27 (s, 1H), 8.01 (s, 1H), 7.83 (d, 1H), 7.70 (t, 3H), 7.46 (m, 4H), 7.21 (d, 2H), 7.07 (m, 4H), 6.74 (m, 1H), 5.80 (d, 1H), 5.30 (d, 1H), 5.13 (s, 2H), 3.97 (t, 2H), 1.80 (t, 2H), 1.48 (m, 2H), 1.36 (m, 4H), 0.94 (t, 3H). Elem. Anal. Calcd. for $\text{C}_{40}\text{H}_{37}\text{N}_3\text{O}_4$: C, 77.02; H, 5.98; N, 6.74; Found: C, 77.04; H, 5.97; N, 6.78. Mp: 268–269 °C.

NA9PH: yield: 61%. $^1\text{H NMR}$ (CDCl_3 , 400 MHz) δ (ppm): 8.79 (s, 1H), 8.64 (m, 2H), 8.27 (s, 1H), 8.02 (s, 1H), 7.85 (d, 1H), 7.71 (t, 3H),

7.46 (m, 4H), 7.21 (d, 2H), 7.03 (m, 4H), 6.74 (m, 1H), 5.80 (d, 1H), 5.30 (d, 1H), 5.14 (s, 2H), 3.97 (t, 2H), 1.81 (t, 2H), 1.48 (m, 2H), 1.31 (m, 10H), 0.92 (t, 3H). Elem. Anal. Calcd. for $\text{C}_{43}\text{H}_{43}\text{N}_3\text{O}_4$: C, 77.57; H, 6.51; N, 6.31; Found: C, 77.55; H, 6.52; N, 6.29. Mp: 262–264 °C.

NA12PH: yield: 61%. $^1\text{H NMR}$ (CDCl_3 , 400 MHz) δ (ppm): 8.75 (s, 1H), 8.62 (m, 2H), 8.22 (s, 1H), 8.02 (s, 1H), 7.80 (d, 1H), 7.71 (t, 3H), 7.40 (m, 4H), 7.19 (d, 2H), 7.01 (m, 4H), 6.72 (m, 1H), 5.80 (d, 1H), 5.26 (d, 1H), 5.11 (s, 2H), 3.96 (t, 2H), 1.79 (t, 2H), 1.45 (m, 2H), 1.27 (m, 16H), 0.89 (t, 3H). Elem. Anal. Calcd. for $\text{C}_{46}\text{H}_{49}\text{N}_3\text{O}_4$: C, 78.05; H, 6.98; N, 5.94; Found: C, 78.01; H, 6.96; N, 5.98. Mp: 249–251 °C.

2.4. Nonlinear optical instruments

2.4.1. Z-Scan measurements

The third-order optical nonlinear properties were measured via the Z-Scan method. The Z-Scan method chooses Nd: YAG nano-second laser as the light source, which owns a wavelength of 532 nm, a pulse width of 4 ns and a repetition rate of 10 Hz. The pulse energy on the sample is 10–20 μJ , the thickness of the sample cell is 2 mm. The measurement can be performed through closed aperture and open aperture configurations.

The optical limiting test was based on the above described Z-scan platform. An attenuator (Newport Co., USA) was fixed at the luminous point of the laser light. The sample was placed at the lens focus. By adjusting the attenuator, the incident energy increases from low to high at a constant rate. During the energy increasing, the incident energy and the outgoing energy were received and recorded by detector D1 and D2, respectively. By a program

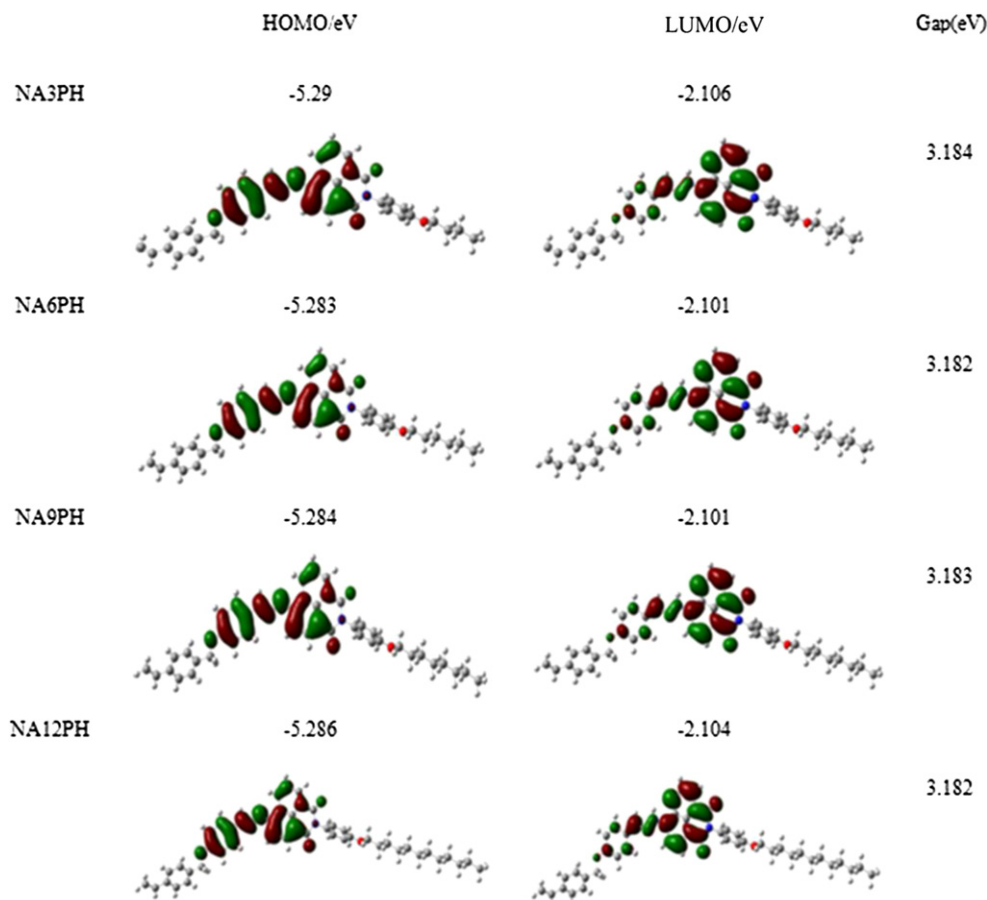


Fig. 3. Electron density distribution of frontier molecular orbital of **NaxPHs**.

manipulation, the change curves of outgoing energy and transmittance with the change of the incident energy can be obtained.

2.4.2. Two-photon excitation fluorescence

The two-photon excitation fluorescence measurements were performed by using an Avesta femtosecond Ti: sapphire oscillator as the excitation source. The output laser pulses have a tunable center wavelength from 750 to 870 nm with pulse duration of 80 fs and a repetition rate of 85 MHz. The samples were dissolved in DMF with the concentration of 2×10^{-5} M and the two-photon fluorescence spectra were measured in the range of 760–870 nm using fluorescein as the reference. The TPA cross section of these four compounds was calculated using the equation:

$$\delta_s = [(F_s \Phi_r C_r) / (F_r \Phi_s C_s)] \delta_r \quad (1)$$

In this equation, subscripts *s* and *r* represent the sample and reference, respectively. *F* is the integral area of the two-photon fluorescence spectra, Φ is the fluorescence quantum yield, *c* is the number density of the molecules in solution and δ is the TPA cross section. The two-photon fluorescence measurements were measured in the region that fluorescence intensity showed a quadratic dependence on excitation laser beam power.

2.4.3. Ultrafast pump-probe measurements

The ultrafast relaxation dynamics of the **NAxPHs** in DMF were measured by using ultrafast transient absorption experiments, which were performed by using a femtosecond Ti: sapphire amplifier laser system (Spectra Physics). The laser pulses were generated from a mode-locked Ti: sapphire oscillator seeded regenerative amplifier with a pulse energy of 2 mJ at 800 nm and a repetition rate of 1 kHz.

3. Results and discussions

3.1. Experimental section

All **NAxPHs** molecules were synthesized via a similar six-step route (Scheme 1) in high yields: 1, 8-naphthalic anhydride was first reacted with aniline to obtain 1,8-naphthalimide. 1,8-naphthalimide further reacted with aromatic aldehyde to obtain the target molecules. Therefore, 1,8-naphthalimide was linked directly with a hydrazone bond. Alkane chain was introduced to

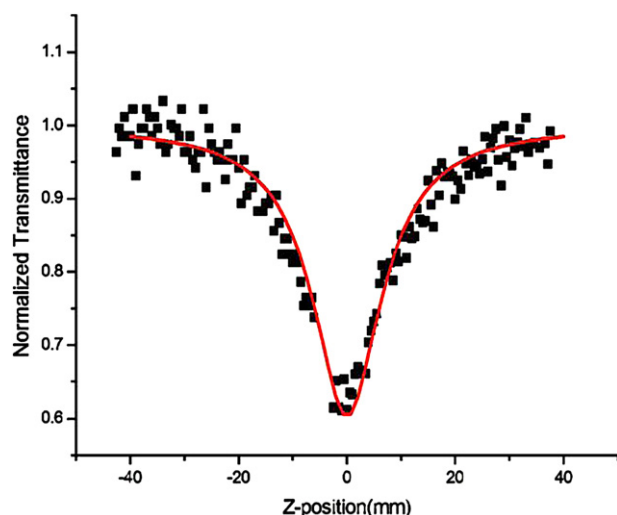


Fig. 4. Z-scan data of **NA3PH** in DMF solution nonlinear absorption of **NA3PH**.

Table 2

Nonlinear optical value of **NA3PH**, **NA6PH**, **NA9PH**, and **NA12PH** in DMF solution.

Sample	$T_0^a(\%)$	$E^b(\mu\text{J})$	$\beta^c(\text{MKS})$
NA3PH	70	3.27	8.76×10^{-9}
NA6PH	70	3.18	8.00×10^{-9}
NA9PH	70	3.29	7.94×10^{-9}
NA12PH	70	3.30	7.53×10^{-9}

^a The linear transmittance.

^b The energy in measurement.

^c Nonlinear absorption coefficient.

enhance the film-forming ability in further fabrication. Moreover, styrene as an electron donor was introduced for providing an active site for polymerization.

The UV–vis spectra of **NAxPHs** in DMF solution were shown in Fig. 1. All of the one-photon absorption spectra exhibit two main absorption bands. The absorption bands at 330 nm and 460 nm are attributed to π – π^* transition of aromatic rings and typical intermolecular charge transfer absorption of 4-substituted naphthalimide, respectively [25].

All molecules exhibit a strong green fluorescence emission. As shown in Fig. 2, the emission spectra exhibit a single broad-band, which indicates that the emission occurs from the lowest excited state with the largest oscillator strength. The emission bands of **NAxPHs** are similar but red shift to 556 nm ($\lambda_{\text{ex}} = 460$ nm) in comparison with naphthalimide group (440 nm). Meanwhile, the intensity of fluorescence is enhanced obviously. This is assigned to the significant ICT and larger conjugation by introducing hydrazone group. The fluorescence quantum yield and fluorescence decay are also measured and the data are collected in Table 1. These compounds possess the similar linear optical properties because of their similar structure. These results can be inferred from theoretical calculations. The electron density distribution of the frontier molecular orbital were shown in Fig. 3. The band gaps of all compounds are similar, ranging from 3.182 to 3.184 eV. In the HOMO of **NAxPHs**, the electrons were distributed throughout the whole molecule. While in the LUMO, the electrons were mainly concentrated on 1,8-naphthalimide. Upon excitation, the electrons were mainly transferred from hydrazone structure to 1,8-naphthalimide, indicating that $-\text{NH}-\text{N}=\text{C}-$ moiety serves as donor for charge transfer.

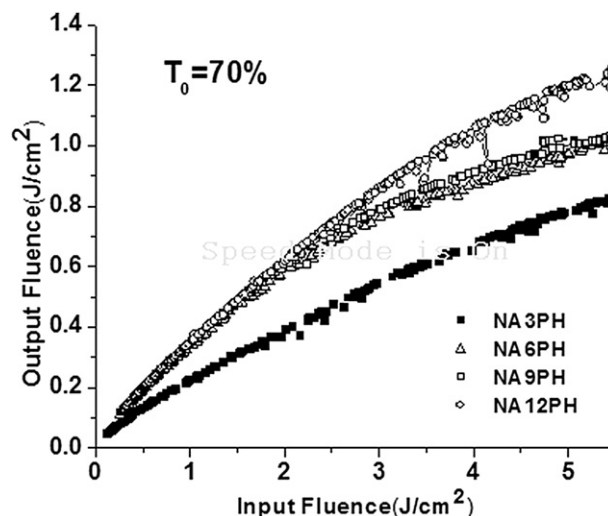


Fig. 5. Optical responses to laser light of **NA3PH**, **NA6PH**, **NA9PH**, **NA12PH** in DMF with a linear transmission of 70%.

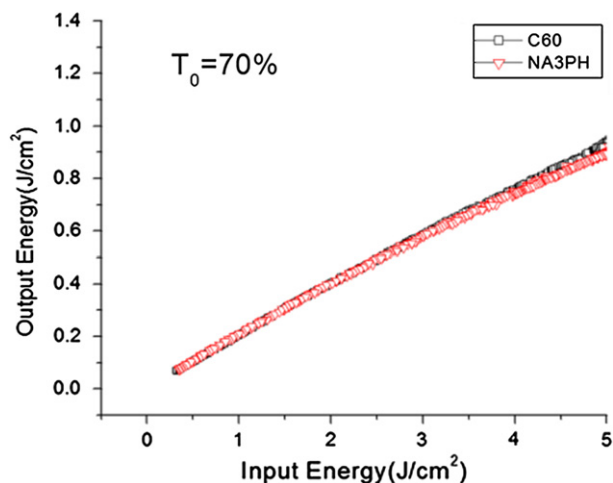


Fig. 6. Optical responses to laser light of NA3PH and C60 with a linear transmission of 70%.

3.2. Nonlinear optical properties for nanosecond laser pulse

The Z-Scan patterns of **NAxPHs** in DMF solution were measured under a wavelength of 532 nm and a pulse width of 4 ns and the linear transmittance of **NAxPHs** were maintained at 70%. Fig. 4 exhibits the nonlinear absorptive pattern of **NAxPHs** and the results demonstrate that all compounds have strong nonlinear absorption. In theory, the normalized transmittance for the open aperture configuration can be written as:

$$T(Z, S = 1) = \sum_{m=0}^{\infty} \frac{[-q_0(Z)]^m}{(m+1)^{1/2}}, \quad \text{for } |q_0| < 1 \quad (2)$$

$$q_0(Z) = \alpha_2 I_0(t) L_{\text{eff}} / \left(1 + Z^2/Z_0^2\right)$$

$$L_{\text{eff}} = [1 - \exp(-\alpha_0 L)/\alpha_0]$$

Where α_2 is the nonlinear absorption coefficient, $I_0(t)$ is the intensity of laser beam at focus ($z = 0$), L_{eff} is the effective thickness with α_0 the linear absorption coefficient and L the sample thickness, z_0 is the diffraction length of the beam, and z is the sample position. The nonlinear absorption coefficient of the **NAxPHs** can be determined by fitting the experimental data of open-aperture Z-scan.

The calculation results of the nonlinear optical coefficients are shown in Table 2. According to Table 2, **NAxPHs** exhibit large nonlinear optical coefficient (β) ranged from 7.53×10^{-9} MKS to 8.76×10^{-9} MKS. Meanwhile, the 4-NHNH₂ naphthalimide did not show any nonlinear absorption phenomenon. The results indicate the nonlinear absorption of these compounds may be attributed to the introduction of hydrazone group based on excited-state absorption (ESA) behaviour. By introducing hydrazone group, highly efficient donor–acceptor pairs were formed, in which naphthalimide as acceptor and hydrazone group as donor. It was proved that optimizing donor and acceptor pairs enhance nonlinear absorption [28,29]. In addition, the resonance structure of hydrazone with naphthalimide group may be also benefit to nonlinear absorption [30]. It's clearly that alkyl chain does not significantly affect the push-pull system and the values nonlinear absorption coefficients are quite close. NLO absorption coefficient slightly decreases from shorter arkyll chain to longer chains. This might be attributed that longer arkyll chain makes the arrangement of chromophore more disordered [31]. Therefore, **NA3PH** behave the largest nonlinear optical coefficient value.

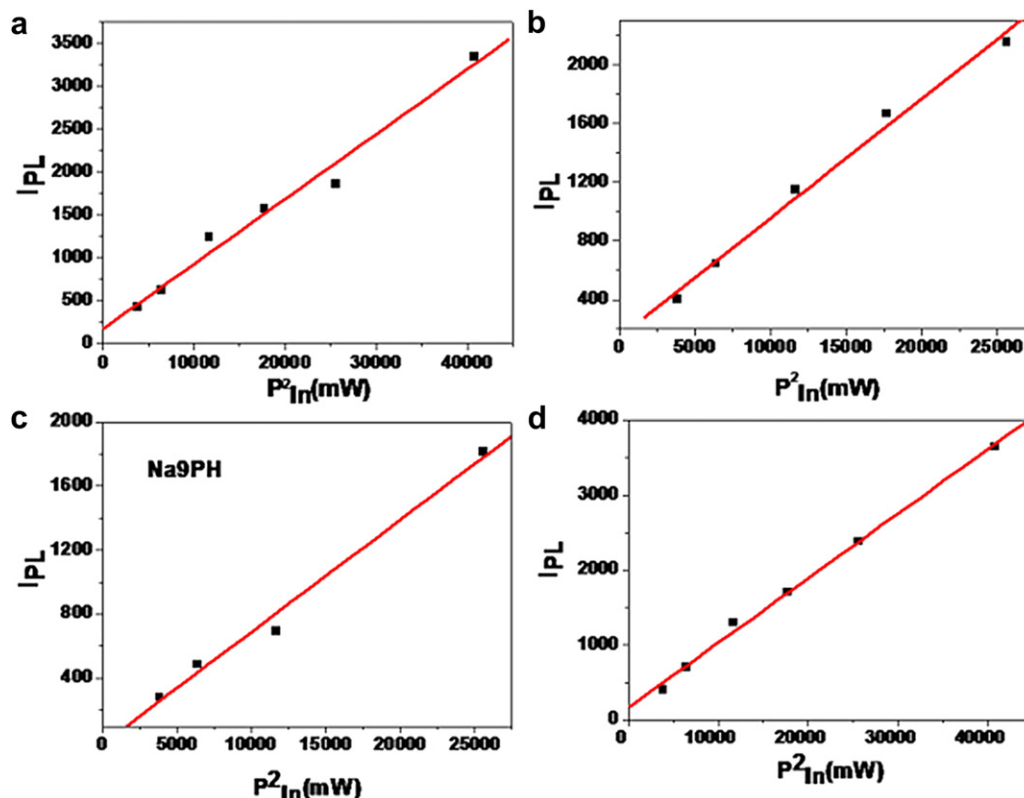


Fig. 7. Dependence of output fluorescence intensity (I_{out}) of NA3PH (a), NA6PH (b), NA9PH (c) and NA12PH (d) on the input laser power (I_{in}) at 800 nm.

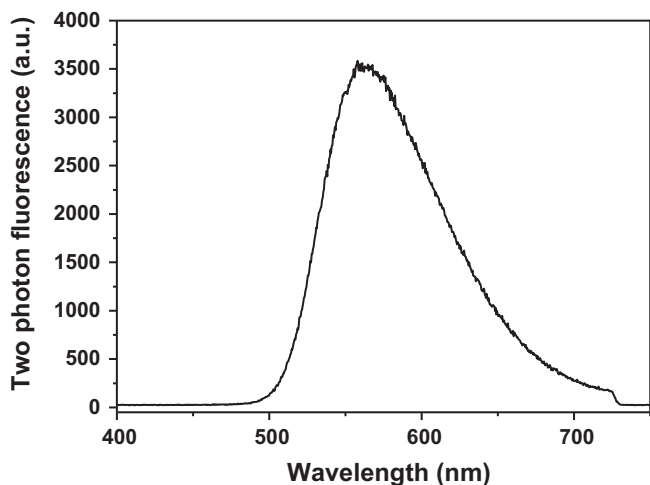


Fig. 8. Two-photon fluorescent spectra of NA3PH.

Fig. 5 shows the optical limiting properties of NAXPHs at the same linear transmittance ($T = 70\%$, $\lambda = 532$ nm) in DMF at the energy range of $1.5 \mu\text{J}$ – $140 \mu\text{J}$. The linear transmittance was measured under the energy of $1.5 \mu\text{J}$. As shown in Fig. 5, when the input fluence further increases, the transmittance starts to decrease, displaying optical-limiting activity. According to Fig. 5, the optical limiting performance of NA3PH is slightly prior to the others, consistent with the results of the nonlinear property analysis.

The optical limiting properties of NA3PH and C₆₀, a benchmark optical limiter, have been compared in this investigation. The results are exhibited in Fig. 6, which show comparable optical limiting properties between NA3PH and C₆₀.

3.3. Two-photon absorption properties for femtosecond laser pulse

Two-photon absorption spectra of NA3PH, NA6PH, NA9PH and NA12PH were measured using two-photon excited fluorescence (TPEF) method in which excitation wavelength was adjusted from 750 to 870 nm. During this process, fluorescein solution (pH = 11) was used as a reference to calibrate the TPEF spectra of these four samples. As can be seen from Fig. 7, two-photon excitation fluorescence intensity of four samples was found to be linear with the square of input laser power, indicating a nonlinear two-photon absorption process.

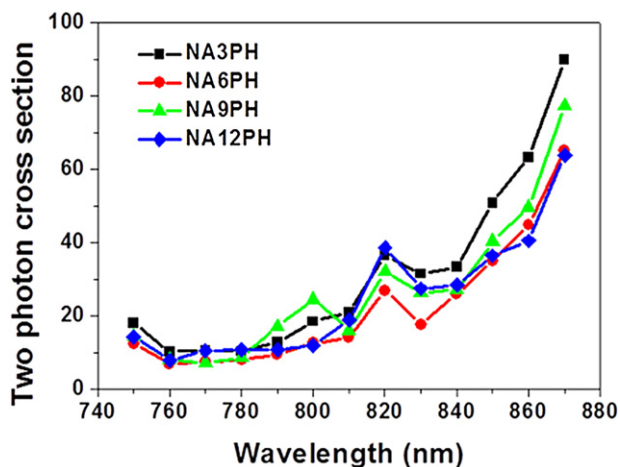


Fig. 9. Two-photon excitation spectra for NA3PH, NA6PH, NA9PH and NA12PH at a concentration of 10^{-5} M in DMF.

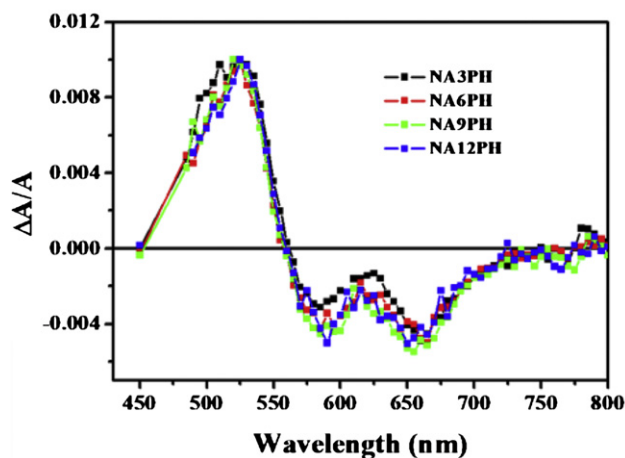


Fig. 10. Femtosecond transient absorption spectra of NA3PH, NA6PH, NA9PH and NA12PH in DMF at 1.0 ps delay time under excitation at 400 nm.

Originated from the 4-substituted naphthalimide, NAXPHs exhibit strong two-photon emission fluorescence (TPEF). TPEF spectra of NA3PH was shown in Fig. 8. Compared with SPEF spectra, one- and two-photon spectra overlap reasonably well and exhibit well defined vibronic structure. The two-photon cross section of these compounds with the same concentration in DMF at different excitation wavelength was shown in Fig. 9 and the data were collected in Table 1. NAXPHs showed moderate two-photon absorption cross section because of its D- π -A configuration. In general, each compound displays a gradual increasing trend in two-photon absorption cross section with the maxima TPA cross-section value of 90 GM for NA3PH, 65 GM for NA6PH, 77 GM for NA9PH and 64 GM for NA12PH. NA3PH behave the largest two-photon absorption cross section, the others are very close. However, due to the similar values of Φ_{max} for NAXPHs, the different results of two-photon absorption cross section are mainly caused by their quantum yields Φ of one-photon fluorescence.

3.4. Ultrafast pump probe measurements

For a detailed understanding of optical limiting mechanisms in these strong push-pull systems (NAXPHs, $x = 3, 6, 9, 12$) in DMF, femtosecond transient absorption measurements have been performed under excitation at 400 nm using femtosecond laser pulses. Fig. 10 shows the transient spectra in the range from 450 to 800 nm at a delay time of 1 ps. It can be seen that the transient features of four compounds are quite similar in DMF. All four compounds display a positive transient absorption between 450 and 560 nm and ground state bleaching in the region of 560–725 nm. The positive transient absorption is due to excited state absorption (ESA, S_1 – S_n). The bleaching in the 560–615 nm regions with a maximum around 590 nm could be ascribing to the stimulated emission. No change in transient absorption spectra was observed by increasing alkyl chain length. It suggests that electronic transition in hydrazone and naphthalene push-pull system is not affected by elongating alkyl chain. All the compounds display strong excited state absorption at 532 nm. The results suggest that excited state absorption contribute significantly to the observed optical limiting effects at 532 nm.

4. Summary

In conclusion, a series of 1,8-naphthalimide derivatives with hydrazone group were synthesized. These compounds show strong excited state absorption at 532 nm using nanosecond laser and

detectable two-photon absorption at 800 nm using femtosecond laser. The pump probe also confirmed the NLO results. Hydrazone bridge plays an important role in the NLO absorption. Elongated alkyl chain length does not improve the nonlinear properties of these compounds but can improve the film-forming ability, which is important for optical limiting device. These compounds can become new dyes in application in broad-band optical limiter. How to further improve their NLO properties by careful molecular design is ongoing in our lab.

Acknowledgements

Authors gratefully thank Chinese Natural Science Foundation No.20876101, 20902065 and 21071105, and major project of college and universities Jiangsu Province (08KJA430004). A Project Funded by the Priority Academic Program Development of Jiangsu Higher Education Institutions.

References

- [1] Areephong J, Kudernac T. On/Off photoswitching of the electro-polymerizability of terthiophenes. *J Am Chem Soc* 2008;130:12850–1.
- [2] He GS, Zhu J, Baev A, Samo M, Frattarelli DL, Watanabe N, et al. Twisted π -system chromophores for all-optical switching. *J Am Chem Soc* 2011;133:6675–80.
- [3] Ehrlich JE, Wu XL, Lee LY, Hu ZY, Rockel H, Marder SR, et al. Two-photon absorption and broad-band optical limiting with bis-donor stilbenes. *Opt Lett* 1997;22:1843–5.
- [4] He GS, Xu GC, Prasad PN, Reinhardt BA, Bhatt JC, Dillard AG. Two-photon absorption and optical-limiting properties of novel organic compounds. *Opt Lett* 1995;20:435–7.
- [5] Shi YQ, Zhang C, Zhang H, Bechtel JH, Dalton LR, Robinson BH. Low (Sub-1-Volt) halfwave voltage polymeric electro-optic modulators achieved by controlling chromophore shape. *Science* 2000;288:119–22.
- [6] Marder SR, Kippelen B, Jen AKY, Peyghambarian N. Design and synthesis of chromophore and polymers for electro-optic and photorefractive applications. *Nature* 1997;388:845–51.
- [7] Jothy VB, Sajjan D, Ravikumar C, Nêmec I, Xia CN, Rastogie VK. First order molecular hyperpolarizabilities and intramolecular charge transfer from the vibrational spectra of NLO material: ethyl-3-(3,4-dihydroxyphenyl)-2-propenoate. *J Raman Spectrosc* 2009;40:1822–30.
- [8] Rath H, Sankar J, PrabhuRaja V. Core-modified expanded porphyrins with large third-order nonlinear optical response. *J Am Chem Soc* 2005;127:11608–9.
- [9] Tykwinski RR, Gubler U, Martin RE, Diederich F, Bosshard C, Günter P. Structure-property relationships in third-order nonlinear optical chromophores. *J Phys Chem B* 1998;102:4451–65.
- [10] Li CW, Yang K, Yan F, Su XY, Yang JY, Jin X, et al. Investigation of two-photon absorption induced excited state absorption in a fluorenyl-based chromophore. *J Phys Chem B* 2009;113:15730–3.
- [11] Anemian R, Morel Y, Baldeck PL, Paci B, Kretsch K, Nunzi JM, et al. Optical limiting in the visible range: molecular engineering around N⁴, N⁴-bis(4-methoxyphenyl)-N⁴, N⁴-diphenyl-4,4'-diaminobiphenyl. *J Mater Chem* 2003;13:2157–63.
- [12] Zhou G, Wang X, Wang D, Wang C, Shao Z, Fang Q, et al. Two-photon absorption and nonlinear optical properties of a new organic dye PSPI. *Opt Commun* 2001;190:345–9.
- [13] Abbotto A, Beverina L, Bozio R, Facchetti A, Ferrante C, Pagani GA, et al. Novel heterocycle-based two-photon absorbing dyes. *Org Lett* 2002;9:1495–8.
- [14] Spangler CW. Recent development in the design of organic materials for optical power limiting. *J Mater Chem* 1999;9:2013–20.
- [15] Chen Y, Hanack M, Araki Y, Ito O. Axially modified gallium phthalocyanines and naphthalocyanines for optical limiting. *Chem Soc Rev* 2005;34:517–29.
- [16] Sun YP, Riggs JE. Organic and inorganic optical limiting materials from fullerenes to nanoparticles. *Int Rev Phys Chem* 1999;18:43–90.
- [17] Bojinov V, Ivanova G, Simeonov D. Synthesis and photophysical investigations of novel polymerizable blue emitting fluorophores—combination of a hindered amine with a benzo[de]isoquinoline-1,3-dione. *Macromol Chem Phys* 2004;9:1259–68.
- [18] Bojinov V, Panova L, Grabchev I. Novel adducts of a 2-(2-hydroxyphenyl)-benzotriazole and a blue emitting benzo[de]isoquinoline-1,3-dione for “one-step” fluorescent brightening and stabilization of polymers. *Polym Degrad Stabil* 2005;3:420–7.
- [19] Srikun D, Miller EW, Domaille DW, Chang CJ. An ICT-based approach to ratiometric fluorescence imaging of hydrogen peroxide produced in living cells. *J Am Chem Soc* 2008;130:4596–7.
- [20] Veale EB, Frimannsson DO, Lawler M, Gunnlaugsson T. 4-Amino-1,8-naphthalimide-based Troger's bases as high affinity DNA targeting fluorescent supramolecular scaffolds. *Org Lett* 2009;18:4040–4.
- [21] Zhang JF, Lim CS, Bhuniya S, Cho BR, Kim JS. A highly selective colorimetric and ratiometric two-photon fluorescent probe for fluoride ion detection. *Org Lett* 2011;13:1190–3.
- [22] Zhao P, Jiang JB, Leng B, Tian H. Polymer fluoride sensors synthesized by RAFT polymerization. *Macromol Rapid Comm* 2009;30:1715–8.
- [23] Lygaitis R, Getautis V, Grazulevicius JV. Hole-transporting hydrazones. *Chem Soc Rev* 2008;37:770–88.
- [24] Lee HY, Song XL, Park H, Baik MH, Lee D. Torsionally responsive C(3)-symmetric azo dyes: azo-hydrazone tautomerism, conformational switching, and application for chemical sensing. *J Am Chem Soc* 2010;132:12133–44.
- [25] Jeong MJ, Park JH, Lee C, Chang JY. Discotic liquid crystalline hydrazone compounds: synthesis and mesomorphic properties. *Org Lett* 2006;8:2221–4.
- [26] Chiwara VI, Haraguchi N, Itsuno S. Polymer-immobilized catalyst for asymmetric hydrogenation of racemic α -(N-Benzoyl-N-methylamino) propiophenone. *J Org Chem* 2009;74:1391–3.
- [27] Gan J, Tian H, Wang ZH, Chen K, Hill J, Lane PA, et al. Synthesis and luminescence properties of novel ferrocene-naphthalimides dyads. *J Organomet Chem* 2002;645:168–75.
- [28] Kang H, Facchetti A, Zhu P, Jiang H, Yang Y, Cariati E, et al. *Angew Chem Int Ed* 2005;44:7922–5.
- [29] Kim T, Kang J, Luo J, Jang S, Ka J, Tucker N, et al. *J Am Chem Soc* 2007;129:488–9.
- [30] Liu BQ, Sun R, Ge JF, Li NJ, Shi XL, Qiu LH, et al. *Dyes Pigm* 2011;88:50–6.
- [31] Vikrant VN, Vasudevan S. *J Phys Chem C* 2011;115:8221–32.